




Special Thermophysical Features of Floor Materials in Mare Smythii Indicated by CE-2 CELMS Data

Cai Liu, Liansheng Mei, Zhiguo Meng , *Member, IEEE*, Yongzhi Wang, Kai Zhu, Weiming Cheng , Zhanchuan Cai , *Senior Member, IEEE*, Jinsong Ping, and Alexander Gusev

Abstract—Mare Smythii is a special basin, which is one of the oldest mare basins with the considerably young mare basalts and the high density of floor-fractured craters. In this article, the microwave sounder, named CELMS, onboard Chang'E-2 lunar orbiter was first invested to assess the thermophysical characteristics of the floor materials in mare Smythii. Based on the numerical simulation with the radiative transfer model and the previous geological results, several special findings are noted as follows. First, the substrate temperature in mare Smythii is likely fairly high, and a special temperature structure is provided. Second, there likely exists an unrevealed deposit in the upper layer of the regolith with strong thermal absorption ability. Third, the CELMS results show a strong correlation with the subsurface features obtained by lunar radar sounder data and the surface wrinkle ridges. These findings will be of essential importance to strengthen knowing the thermal and magmatic evolutions of the lunar maria.

Index Terms—High substrate temperature, mare Smythii, microwave propagation, remote sensing, thermal anomaly, wrinkle ridges.

Manuscript received March 7, 2021; revised June 10, 2021, July 13, 2021, and July 30, 2021; accepted August 1, 2021. Date of publication August 10, 2021; date of current version August 30, 2021. This work was supported in part by the B-type Strategic Priority Program of the Chinese Academy of Sciences under Grant XDB41000000, in part by the National Natural Science Foundation of China under Grant 42071309, in part by the opening fund of State Key Laboratory of Lunar and Planetary Sciences (Macau University of Science and Technology) (Macau FDCT Grant 119/2017/A3), and in part by the Science and Technology Development Fund of Macau under Grant 0059/2020/A2 and Grant 0052/2020/AFJ. (*Corresponding authors: Zhiguo Meng; Yongzhi Wang.*)

Cai Liu, Liansheng Mei, Zhiguo Meng, and Yongzhi Wang are with the College of Geoexploration Science and Technology, Jilin University, Changchun 130026, China, with the State Key Laboratory of Lunar and Planetary Sciences, Macau University of Science and Technology, Macau 999078, China, and also with the Key Laboratory of Lunar and Deep Space Exploration, National Astronomical Observatory, CAS, Beijing 100012, China (e-mail: liucaijlu.edu.cn; meils20@mails.jlu.edu.cn; mengzg@jlu.edu.cn; wangyongzhi@jlu.edu.cn).

Kai Zhu is with the Institute of Geochemistry, Chinese Academy of Sciences, Guiyang 550081, China (e-mail: zhukai@mail.gyig.ac.cn).

Weiming Cheng is with the State Key Laboratory of Resources and Environmental Information System, Institute of Geographic Sciences and Natural Resources Research, Chinese Academy of Sciences, Beijing 100101, China (e-mail: chengwm@reis.ac.cn).

Zhanchuan Cai is with the Faculty of Information Technology and State Key Laboratory of Lunar and Planetary Sciences, Macau University of Science and Technology, Macau 999078, China (e-mail: zccai@must.edu.mo).

Jinsong Ping is with the Key Laboratory of Lunar and Deep Space Exploration, National Astronomical Observatory, CAS, Beijing 100012, China (e-mail: jsping@bao.ac.cn).

Alexander Gusev is with the Institute of Geology, Kazan Federal University, Kazan 420008, Russia (e-mail: alexander.gusev@mail.ru).

Digital Object Identifier 10.1109/JSTARS.2021.3103888

I. INTRODUCTION

MARE Smythii, centered at (87 °W, 2 °S), is one of the most ancient regular impact basins with multiple ring structures [see Fig. 1(a)]. It is located at the eastern limb of the lunar nearside, which extends from the main mare regions in the west part (lunar nearside) to the highlands in the east part (lunar farside). Mare Smythii contains valuable information about the primary and secondary crustal formation processes on the Moon [1]–[4]. Therefore, the study on mare Smythii can provide fundamental information about the thermal and magmatic evolutions of the Moon.

Until now, mare Smythii has been thoroughly studied with the Lunar Orbiter, Apollo photographs, Apollo X-ray data, Clementine ultraviolet-visible (UV/VIS), gravity, and topography data [1]–[5]. It is one of the most geologically diverse areas, which has the rather old basin floor deposit in the southwest interior and fairly young mare deposits in the northeast interior of the basin [3], [6] [see Fig. 1(b)]. Moreover, there exist abundant isolated craters in mare Smythii, which are partly filled with the basalt in the crater floor [3], [6]. Also, Wilhelms *et al.* mapped a high concentration of floor-fractured craters in the southwestern part of Smythii basin, and the concentration is nearly highest among the lunar maria [7]. What's more, Gillis and Spudis thoroughly analyzed the distribution of the floor deposits in mare Smythii with the Clementine UV-VIS data [3]. Recently, with the SELENE lunar radar sounder (LRS) data, Ishiyama and Kumamoto attributed the basin floor deposits to the mare deposits in the early stage, which covered the whole basin floor including the substrate layer beneath the young mare unit in the northeast interior [8]. This brings a new view of the floor deposits in mare Smythii and, therefore, it is necessary to further study mare Smythii with more sources of data.

Comparatively, carried by Chang'E (CE) -1 and -2 lunar orbiters, one of the main payloads is the microwave sounder (CELMS), which worked in the pattern of passive microwave remote sensing. The CELMS data bring a new method to assess the thermal emission features of the materials on the lunar surface. The CELMS instrument operated at four channels, 3.0, 7.8, 19.35, and 37.0 GHz, respectively, reflecting the thermophysical characteristics of volumetrically lunar regolith in four corresponding depths [9]–[11]. Moreover, the data have been proven to be highly correlated to the thermophysical characteristics of the volumetric regolith in certain depth, which is partially decided by the thermal state of the shallow lunar crust

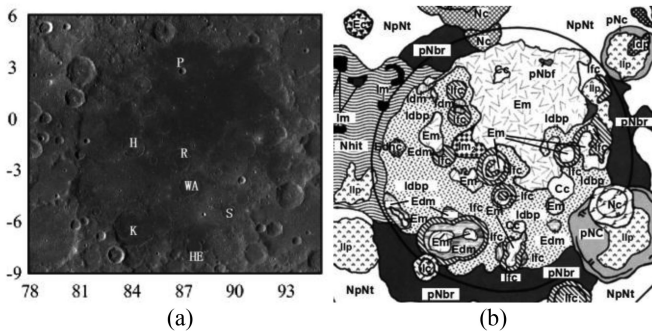


Fig. 1. (a) Mosaic of optical images from LROC showing the geography of Smythii basin: Haldane (*H*); kiess (*K*); peek (*P*); runge (*R*); swasey (*S*); and warner (*WA*) (the unit is given in decimal degree, geological coordinate system). (b) Geological map of Smythii [3]. The solid line indicates the crest of basin ring.

and compositions of the volumetric regolith [10], [12]–[16]. Also, in such depth, the material is less influenced by the space weathering and less contaminated by the ejecta from the impact event in the distance [10], [12]–[16]. Thus, the CELMS data postulate a unique way to evaluate the floor materials within and surrounding mare Smythii.

Further, besides the substrate temperature and the regolith compositions, the CELMS data has been widely accepted to be heavily affected by the surface temperature, which is significant varied with the latitude and surface topography [10], [14], [15] [17]–[19]. Interestingly, mare Smythii is just positioned in the low latitude region, and the variation of the surface temperature in the north-southern direction is slight [13], [17], [20]. Additionally, after evaluating the brightness temperature (TB) performances in Hertzsprung region, Meng *et al.* [21] thought that the surface topography plays a negligible role on the observed CELMS data in the low latitude regions in macroscale. That is, mare Smythii is an appropriate candidate to highlight the relationship between the thermophysical characteristics of the floor materials and the CELMS data, which is also the motivation for us to promote this work.

In the article, the CELMS data from CE-2 lunar orbiter are applied to assess the thermophysical characteristics of the floor materials in mare Smythii. Section II presents the process procedure of the CE-2 CELMS data and the Clementine UV/VIS data. Section III provides the thermophysical features of the main geological units and the problems revealed by TB performances. Section IV is to solve the problems about the special TB performances of the floor materials in mare Smythii, and the conclusions are provided in Section V.

II. DATA PROCESSING

The CE-2 CELMS data and the Clementine UV-VIS data are employed in this article.

A. CELMS Data Processing

The CELMS data are processed to obtain the TB maps, which are then used to assess the thermophysical characteristics of the floor materials in mare Smythii. The

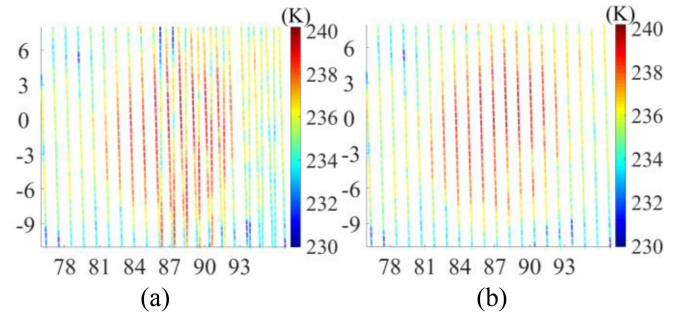


Fig. 2. Scatter plots of the selected TB points (3.0 GHz) at 12:00-13:00. (a) original sampling data. (b) TB points only including sample one (the unit is given in decimal degree, geological coordinate system).

description of the CE-2 CELMS data can be referred to Zheng *et al.* [10], [14] and Cai and Lan [22], and Meng *et al.* [11], [15], [21].

1) *TB Maps Generation*: The generation of the TB maps has been thoroughly described by Zheng *et al.* [10], [14], Cai and Lan [22], and Meng *et al.* [15], [16], [19], which is adopted in this article. First, the TB points in the geographical range of mare Smythii are chosen, which are ascribed into 24-h intervals using the hour angle method. Second, the scatter plots of the selected TB points in the 24-h intervals are compared, and the CELMS data in the time intervals from 12:00 to 13:00 and from 21:00 to 22:00 are appropriate to express the thermophysical feature of the regolith at daytime and night, respectively [see Fig. 2(a), daytime TB points].

Here, a new phenomenon should be strengthened, which has not been encountered before. Fig. 2(a) shows that there exist TB points in two different global coverages. Here, we defined the coverage including the whole study area to be Sample One and that only comprising the eastern part of the study area to be Sample Two. According to the identical distance between the two adjacent tracks, Sample Two is only located in the orbits from 86 °E to 95 °E, including ten tracks. However, the values of Sample Two are clearly higher in the southern part but lower in the northern part of the study area than that of Sample One. Comparatively, Fig. 2(a) expresses that the TB values of Sample One are similar in the neighboring tracks along the same latitude, therefore indicating the rationality of these data. Thus, the TB points in Sample Two are eliminated, and only Sample One is kept as shown in Fig. 2(b).

Finally, the linear interpolation method was adopted to make continuous TB maps with a $0.25^\circ \times 0.25^\circ$ spatial resolution (see Fig. 3).

Fig. 3 shows an apparently higher TB in the Smythii floor compared to the surrounding highlands. Besides, the craters Peek, Swasey, and Warner indicate a good correlation with the abnormally low TB values both at daytime and at night, implying the rationality of the generated maps at least in geographical position. To clear understand the TB performances of the floor materials, we vectorized the geological map in Fig. 1(b) and overlaid the boundaries on the generated TB maps, which are shown in Fig. 4(daytime) and Fig. 5(night). The solid lines

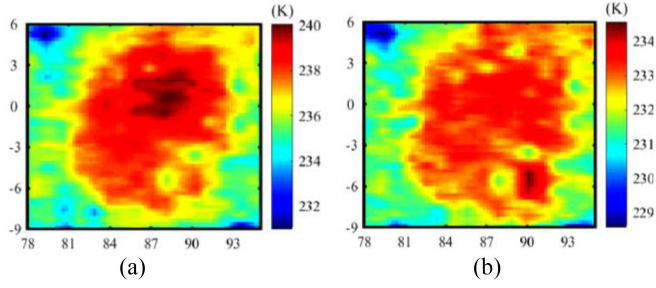


Fig. 3. TB maps of mare Smythii at 3.0 GHz. (a) Daytime. (b) Night (the unit is given in decimal degree, geological coordinate system).

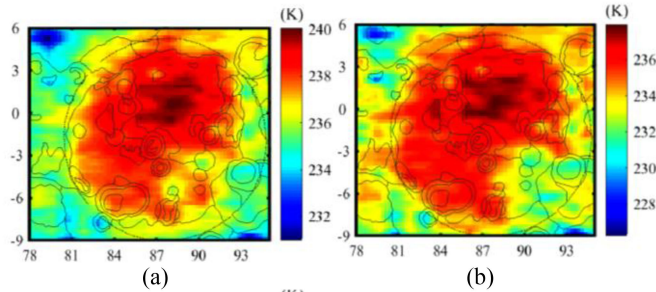


Fig. 4. TB maps of mare Smythii at noon. (a) 3.0 GHz. (b) 7.8 GHz. (c) 19.35 GHz. (d) 37 GHz (the unit is given in decimal degree, geological coordinate system).

indicate the geological boundaries and the dashed line indicates the crest of Smythii basin ring in the following figures.

2) *Generating TB Difference Maps*: The TB difference, named dTB, is postulated as the difference between the TB values of the same frequency generated in two different hour angles, which indicates a well description of the thermophysical characteristics of the mare deposits in the wavelength-related penetration depth [19], [23], [24]. Thus, the dTB maps are created using the interpolated daytime and night TB data in the previous step (see Fig. 6).

The rationality of the generated maps is evaluated by comparing our results to the global TB maps provided by Chan *et al.* [18], Zheng *et al.* [10], [14], and Cai and Lan [22] using the CE-1/2 CELMS data. The TB maps in Figs. 4 and 5 show good agreements with previous results in global scale [10], [14], [18], [22]. Moreover, the TB maps at the time intervals from 5:00 to 6:00 and from 9:00 to 10:00 are also generated, which present similar local performances. These comparisons validate that the TB and dTB maps in mare Smythii are reliable.

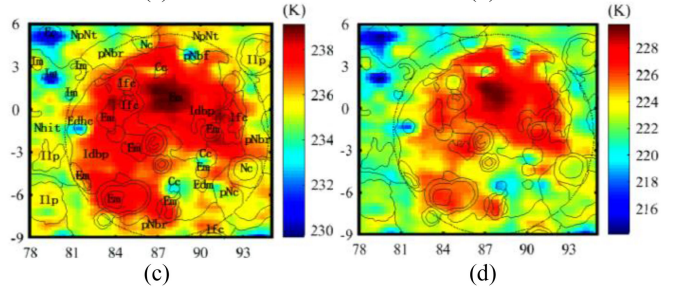
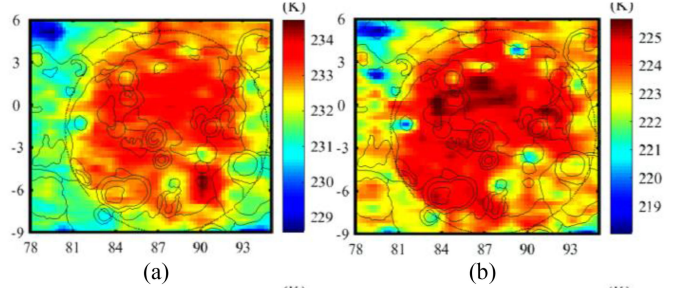


Fig. 5. TB maps of mare Smythii at night. (a) 3.0 GHz. (b) 7.8 GHz. (c) 19.35 GHz. (d) 37 GHz (the unit is given in decimal degree, geological coordinate system).

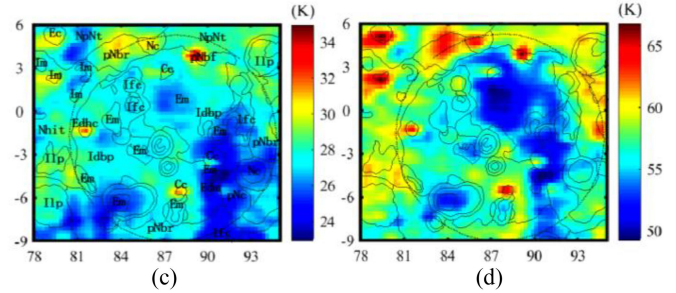
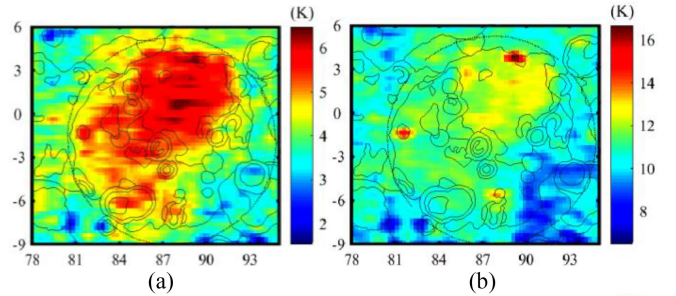


Fig. 6. dTB maps of Mare Smythii. (a) 3.0 GHz. (b) 7.8 GHz. (c) 19.35 GHz. (d) 37 GHz (the unit is given in decimal degree, geological coordinate system).

Moreover, as mentioned in Section I, the TB performances in Figs. 4 and 5 show a negligible correlation with the surface topography, for no crater walls present the abnormal TB performances related to the topography. Meanwhile, the variations of the TB values with latitude are slight, as is indicated by the TB values in the west highlands along the longitude. That is, the relationship between the regolith thermophysical parameters and the CELMS data can be highlighted, which is helpful to pursue the fundamental characteristics of the floor materials in mare Smythii.

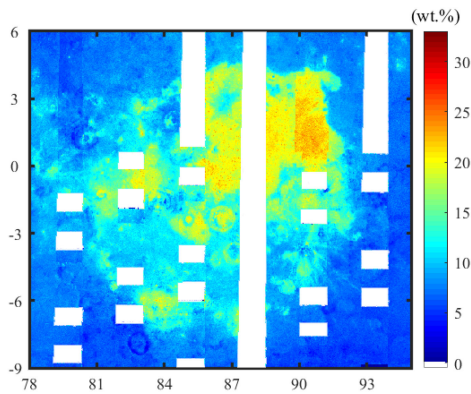


Fig. 7. FTA map of mare Smythii (the unit is given in decimal degree, geological coordinate system).

B. Clementine UV-VIS Data

In order to better understand TB and dTB behaviors in mare Smythii, the $(\text{FeO} + \text{TiO}_2)$ abundance (FTA) related to the surface materials is calculated. The methods designed by Lucey *et al.* [25] are applied to invert the FeO and TiO_2 contents using the Clementine UV/VIS data (see Fig. 7), which were downloaded from the U.S. Geological Survey site.¹

Fig. 7 shows that the FTA is highest in the northeast interior and abundant isolated large craters [Em unit in Fig. 1(b)], moderate in southwest Idbp unit, and lowest in other units and the surrounding highlands. Compared to the TB and dTB maps, Fig. 7 shows a special understanding of the TB and dTB performances in mare Smythii combined with the theoretical simulations.

III. RESULTS

Gillis and Spudis systematically studied the geological features of mare Smythii and presented 22 geological units within and surrounding Smythii basin [3]. Considering the low spatial resolution of the original CELMS data and the limited area of the abundant geological units, only the Eratosthenian mare materials (Em unit), Imbrian dark basin plains (Idbp unit), and highland material (Nectarian or preNectarian undivided terra, NpNt unit) are the main focuses in this article.

A. TB and dTB Performances of Geological Units

The Em unit is the mare deposit filling the northeast interior of Smythii basin and forming isolated ponds within some of the modified floor-fractured craters, which is characterized by high FTA values, smooth surface, and low crater densities [3] (see Fig. 1). The Idbp unit includes the material occupying the southwestern and central floor of Smythii basin (see Fig. 1). It is intermediate in albedo and FTA values between mare and adjacent highland terra [3].

Fig. 4 shows that, at noon, the TB of the mare deposit is highest at 3.0 and 7.8 GHz in the central part of the northeast Em unit, while the differences between the unit and the nearby

Idbp and NpNt units are not apparent. At 19.35 GHz, the TB in the whole northeast Em unit is homogeneously high as the nearby Idbp and NpNt units. However, at 37 GHz, the TB of the northeast Em unit is about 3 K lower than the floor units in the western Idbp unit.

At night, the TB of the majority part of the Em and Idbp units is homogeneously high within Smythii basin at 3.0, 7.8, and 19.35 GHz channels. Apparently, from the 7.8-GHz frequency, the highest TB occurs in the central part of the northeast Em unit. It is geographically identical to the regions with the highest 3.0- and 7.8-GHz daytime TB, while the range is slightly smaller than that in the daytime TB maps. Additionally, at 37 GHz, the TB of the northeast Em unit is about 3 K higher than the floor units in the western interior.

The dTB maps indicate the highest values in the north interior at 3.0 GHz, whose range includes the majority of the northeast Em unit and extends to the southwest Idbp unit. At 7.8 GHz, the dTB of the northeast Em unit is shown to be higher than the rest of the basin floor. At 19.35 GHz, except for the central part with low values, the dTB of the majority part of the northeast Em unit is homogeneously high as the nearby Idbp unit. However, at 37 GHz, the dTB of the northeast Em unit becomes apparently lower than the Idbp unit in the western interior. Here, the central part of the northeast interior should be paid attention to, which gives the lowest dTB at 7.8, 19.35, and 37 GHz maps within the unit and the lowest dTB at 37 GHz within Smythii basin.

Aside from the continuous mare deposit in the northeast interior, Yingst and Head outlined 25 lava ponds within Smythii floor, which is marked as Em or Edm (Eratosthenian dark mantle material) units [1]. However, except craters Kiess (84.1 °E, 6.4 °S) and Swasey (89.7 °E, 5.5 °S), no special TB and dTB performances occur in these lava ponds. The TB and dTB performances in Kiess crater are similar to those in the northeast interior, while their performances in Swasey crater are always the lowest among the basaltic units within the basin floor.

The NpNt unit is rich in plagioclase, which is the dominant geological unit outside the innermost ring of Smythii basin. The unit is characterized by the low FTA values, complex surface, and wide-spread craters [3]. In the study area, NpNt unit mainly occurs in the four corners of the study area. Figs. 4–6 indicate complex TB and dTB performances in NpNt unit. For the area of the unit is small, it is also not the main focus of this article. The TB performances are used for reference when evaluating the thermophysical features of Em and Idbp units.

Besides the above mentioned Em, Idbp, and NpNt units, there also exist the pyroclastic deposits (Eratosthenian and Imbrian dark mantle materials, Edm and Idm units) and Imbrian mare materials (Im and Im2 units). However, it is difficult to identify them from their vicinities for the small areas of the units. Thus, the units of such kinds are not considered in the following discussions.

B. Problems Revealed by TB Performances

To clear understand the special thermophysical characteristics of the floor materials, the microwave radiative transfer model is constructed to express the normal change of the simulated TB

¹[Online]. Available: http://webgis.wr.usgs.gov/pigwad/download/moon_dl.htm

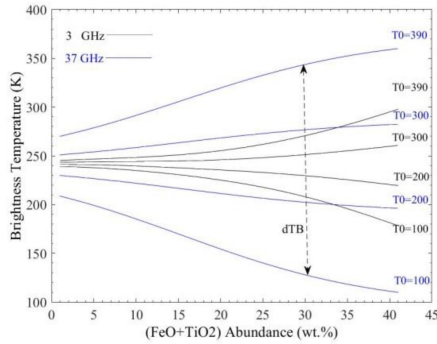


Fig. 8. Change of simulated TB with FTA and surface temperature [11].

with the compositions of the surface deposits on conditions of different surface temperatures. Here, the layered regolith-rock model is employed to solve the radiative transfer equation and the regolith parameters are adopted similar to the reference [11], [26] (see Fig. 8).

However, compared to the simulation result in Fig. 8, Figs. 4–6 indicate that the TB performances are rather abnormal, which is beyond our current knowledge about the thermophysical characteristics of the floor materials in mare Smythii. There are three problems that are hard to understand.

1) *Relationship Between the TB Behaviors and the FTA of the Floor Materials Does not Agree With the Simulation Result:* Based on the numerical simulation results, the regions with higher FTA should always have a higher TB at daytime and a lower TB at night than those with lower FTA [11], [26]. Generally, the FTA is highest in Em unit, followed by Idbp unit and NpNt unit. Theoretically, the daytime TB should be highest in Em unit and lowest in NpNt unit, and it is converse at night. Correspondingly, Fig. 4 shows that this phenomenon is right at 3.0 and 7.8 GHz. However, Fig. 4 (d) shows that the daytime TB at 37 GHz is lower in Em unit with higher FTA than those in Idbp unit with moderate FTA and in NpNt unit with the lowest FTA. Moreover, Fig. 5 presents that the TB at night is unexpectedly the highest in Em unit and the lowest in NpNt unit. Such TB performances are entirely different from the simulation results.

As a whole, the TB within the Smythii floor is apparently greater than the highland unit with the lowest FTA no matter at noon and night.

According to the TB performances in maria Nubium, Moscoviense, and Orientale [11], [26], [27], such TB performances likely mean the existence of the hot anomaly in the substrate of the lunar regolith. The special TB performances in mare Smythii give a new view of the hot substrate anomaly.

2) *Change of the TB With Frequency is Abnormal:* Based on the theoretical simulation, the deposits with higher FTA should always have a higher TB at daytime, and the difference becomes enlarged with the increasing of the frequency. Theoretically, compared to the deposits with lower FTA values, the deposits with higher FTA will have the highest daytime TB and a lowest night TB at 37 GHz, followed by 19.35, 7.8, and 3.0 GHz.

However, the TB performances in northeast Em unit are abnormal. First, as the region with the highest FTA in mare Smythii, Fig. 4 shows that the daytime TB in Em unit is higher

at 3.0 and 7.8 GHz compared to that in Idbp unit, as is reasonable based on the theoretical simulation. But at 37 GHz, the TB in Em unit is apparently lower than that in Idbp unit, which is contrary to the simulation results. Also, the dTB performances validate this abnormal phenomenon, where the dTB values in Em unit are higher at 3.0 and 7.8 GHz but lower at 37 GHz than those in Idbp unit. Second, at night, there exists a small patch with the highest TB in the northeast Em unit, and the area of the patch clearly changes with the frequency. Moreover, in the southeast margin of Idbp unit centered at Swasey crater, the daytime TB is similarly high as the remaining part of Idbp unit, while it becomes the lowest in other channels. Particularly at 37 GHz, the region with the lowest TB extends along the north-south direction and ends in the north boundary of the Smythii floor, which occupies the majority part of Em unit. At night, the TB in the region is almost highest at 3.0 GHz, while it is approximate to the nearby regions at 7.8 GHz, and it is apparently lower than the nearby region at 19.35 and 37 GHz.

Such special TB and dTB performances not only mean the variation of the thermophysical parameters of the regolith in vertical direction, but also hint the existence of the material with abnormal thermophysical features.

3) *TB Performances in the Northeast Em Unit is Special:* Clearly, there exists a special region in the central part of Em unit in the northeast interior of the Smythii floor. The region is largely centered at (88 °E, 1 °N) with a diameter of about 90 km. It indicates the highest TB at 3.0 and 7.8 GHz at daytime and at 7.8, 19.35, and 37 GHz at night. However, it presents the lowest daytime TB at 37 GHz. The dTB maps also verify the existence of the special region, which postulates the lowest values at 7.8, 19.35, and 37 GHz.

Besides the hot substrate anomaly, we have not encountered such special TB performances in other regions of the lunar surface until now, and these findings will be further discussed in the following Section.

IV. NEW UNDERSTANDING OF MARE SMYTHII

This section is tried to solve the above mentioned three problems.

A. Hot TB Anomaly in Basin Floor

The goal of this part is to solve the aforementioned first problem, to pursue the reasons for the inconsistencies between the TB performances and the simulation results.

Figs. 4 and 5 show that the TB in Em unit with elevated FTA is higher than that in Idbp unit with moderate FTA, which is rational according to the simulation results. But, the daytime TB values at 37 GHz in Em unit are clearly lower than those in Idbp region, as is not rational. Particularly, the FTA values in Smythii floor are apparently larger than the nearby highland NpNt unit, while the TB in the former is higher than the latter both at daytime and night.

Similar findings also occur in maria Nubium, Moscoviense and Orientale [11], [26], [27]. Currently, Chan *et al.* [18], Zheng *et al.* [10], [14], Fang and Fa [13], and Hu *et al.* [17] accepted the great influences of the FTA, surface slope, and rock abundance

Em	Idbp	Unit
T ₁	T ₂	shallow layer
T ₃	T ₄	deep layer

Fig. 9. Temperature structures at daytime outlined in mare Smythii (the shallow layer is about 10 cm thick in Em unit and no more than 20 cm thick in IDBP unit.).

on the TB performances of the surface deposits. Here, the influence of the FTA is eliminated because the observed night TB is just opposite to the theoretical simulation. The surface slope can also be omitted because the region with TB anomaly is just located within the low latitude region with almost the subsolar illumination at noon. Finally, the rock abundance is excluded for Zheng *et al.* [10], [14], Hu *et al.* [17], and Meng *et al.* [16], [21] suggested that the TB will become lower at night in the regions with abundant rocks, opposite to the observation in mare Smythii.

To further assess the genesis of the hot TB anomaly, Meng *et al.* [11] ascribed the phenomenon to the high substrate temperature, or internal thermal flux based on the theoretical model, for it is one of the key parameters to obtain the temperature profile with the thermal conduction model. Keilm [12] also proposed the probability of the passive microwave data in acquiring the internal thermal flux of the Moon. Thus, the only hypothesis is that there exists a high substrate temperature in mare Smythii, which causes the high TB at night in the regions with high FTA.

However, this hypothesis is hard to grasp by the daytime TB performance at 37 GHz, which is lower in Em unit with the highest FTA than that in the nearby Idbp unit and even the highland NpNt unit. Fortunately, this special TB performance validates the rationality of the hypothesis. Considering the penetration depths of the used microwave, a temperature structure can be constructed in Smythii, as shown in Fig. 9.

The penetration depth of the CELMS data declines with the increase of the frequency. Therefore, Fig. 9 is outlined to simply describe the equivalent temperature structures of the lunar regolith at daytime in Em and Idbp units. Here, T₁ and T₂ represent the equivalent temperatures in the upper layer indicated by the 37-GHz microwave, while T₃ and T₄ represent the equivalent temperatures within the lower layer penetrated by the microwaves at 3.0 and 7.5 GHz. As is shown in Fig. 4, the daytime TB in Em unit is apparently lower than that in Idbp unit at 37 GHz, while the former is apparently higher than the latter at 3.0 and 7.8 GHz. Correspondingly, the lower daytime 37-GHz TB value in Em unit means that T₁ is lower than T₂ in the shallow layer. If this is so, to obtain the relatively higher nighttime TB in Em unit at 3.0 and 7.8 GHz, T₃ should be much higher than T₄. Only under this condition can the TB be higher in Em unit than that in Idbp unit according to the theoretical model. Therefore, the hypothesis about the high substrate temperature in mare Smythii is possible.

Theoretically, the TB in Em unit with the highest FTA should be much lower than that in Idbp unit at night according to the

simulation results. However, the observed TB is actually shown to be highest in Em unit. This again validates that the substrate temperature is fairly high, particularly beneath Em unit in the northeast interior. What's more, the TB values in Smythii floor are also apparently larger than the nearby highland NpNt unit both at noon and at night except at noontime 37-GHz map, similar as the TB performances in Em and Idbp units. This means that the substrate temperature in Smythii floor is abnormally high as a whole. The hot TB anomaly in such size is rare over the lunar surface, which has great significance in studying the thermal evolution of the Moon.

Besides the TB anomaly in Em unit, we mentioned that there also occur abnormal TB performances in the regions centered at (90 °E, 4 °N), (88 °E, 6 °S), and (80 °E, 2 °S), which is clearly expressed in the dTB map at 7.8, 19.35, and 37 GHz. Fig. 5 shows comparatively lower values at night, while Fig. 4 shows that they are very high at 37 GHz but relatively lower at 3.0 and 7.8 GHz at daytime. After comparing the TB behaviors and the rock abundances, Meng *et al.* [16], [21] ascribed the TB anomaly of such kind to the existence of rocks, which is not further discussed in this article.

B. Revealed Special Floor Material

The goal of this part is to solve the aforementioned second problem, to pursue the reasons for the special variation of the TB in the four channels.

Considering that the CELMS data have been proposed to be highly correlated to the thermophysical characteristics of the mare deposits within the penetrated depth [9], [16], [19], [23], [28], the variations of the TB values with frequency probably mean the changes of the thermophysical parameters of the volumetric regolith in the vertical direction. But, considering the existence of the hot anomaly mainly beneath Em unit, the dTB maps are employed to assess the phenomenon, and the TB maps are used for references.

Until now, the variation of volumetric regolith thermophysical features with depth has not been reported by other studies with the remote sensing techniques. To clearly understand the issue, we first assume that the thermophysical parameters of the volumetric regolith are constant with depth, if the dTB of the deposits does not change with frequency compared to its nearby regions. This assumption can be verified by the dTB performances in Idbp unit. Apart from Swasey, Haldane, and Kiess craters, the fluctuations of the TB values are rather small and the values keep constant compared to the nearby highlands. The even distribution of the dTB values hints the homogeneity of the thermophysical parameters of volumetric regolith from the deep to the shallow layers.

Then, if the dTB of one region clearly changes with frequency compared to its nearby regions, we assume that it is likely caused by the variations of the thermophysical parameters of the lunar regolith in vertical direction. Fig. 6 shows a good description of the assumption in Em unit combined with Figs. 4 and 5. Here, the dTB is highest at 3.0 and 7.8 GHz, however, it becomes relatively lower at 19.35 GHz in the central part, and it becomes nearly the lowest at 37 GHz in the majority of the unit. According

to the simulation results, this means that the FTA is rich in the substrate layer represented by the 3.0 and 7.8 GHz microwave. However, it is hard to accept that the FTA is absent in the shallow layer indicated by the microwave at 19.35 and 37 GHz, for the outmost layer of the regolith is also rich in FTA indicated by the optical results in Fig. 7.

The probable cause of these findings is the occurrence of a special material in the upper layer of the regolith in Em unit, which is strong in the thermal absorption ability. This hypothesis can be verified by the relatively lower 37-GHz TB during the daytime and the highest 7.8-, 19.35-, and 37-GHz TB at night.

Additionally, we mentioned the special TB and dTB performances in the east margin of Idbp unit centered at Swasey crater. It indicates the lowest dTB values in the central part and relatively lower dTB values in the surrounding region, which is similar to the special dTB performance in Em unit at 37 GHz. This means that the materials in the two regions should be identical. Thus, the region with the special material comprises the eastern part of the Smythii floor, and it extends from the southeastern boundary of mare Smythii to the northern boundary.

What's more, according to the dTB performances, the special material also exists in Kiess crater, the west part of Runger crater (86.8 °E, 2.4 °S), and the north and west parts of Haldane crater (84.1 °E, 1.7 °S).

Since the regolith in mare Smythii is rich in ilmenite content, the microwave signal can only reflect the regolith to about ten times of the wavelength [9]. Thus, considering that the dTB performance in Em unit is abnormal only at 19.35 and 37 GHz and it is normal at 3.0 and 7.8 GHz, this special material occurs in the depth less than 38.5 cm (penetration depth of 7.8-GHz microwave), but larger than 16.5 cm (penetration depth of 19.35-GHz microwave).

Such special material is also not reported until now. More work should be done to further understand the origin and its geological meanings of the material.

C. Special TB Performances in EM Unit

The goal of this part is to solve the aforementioned third problem, to pursue the cause for the hot TB anomaly centered at (88 °E, 1 °N) with a diameter of about 90 km. It is located in the central part of the extensive young mare unit. Until now, no TB of such kind has been reported.

For there is absent in visible flow fronts, crater density, uniform spectral feature, and iron and titanium concentrations of the main basalt deposit, Gillis and Spudis hypothesized that the northeast Em unit was deposited in a single eruptive event and from a single source at depth [3]. Also, they inferred that eruptions occurred in the northeast and flowed to the west and southwest according to the topographic features of the main basalt deposit, though the unit is absent in any obvious volcanic surface features.

However, this hypothesis cannot be supported by the TB and dTB maps, for there are not any special TB and dTB performances in the northeast Em unit. Conversely, the shape and the surface features hint that the abnormal TB region has

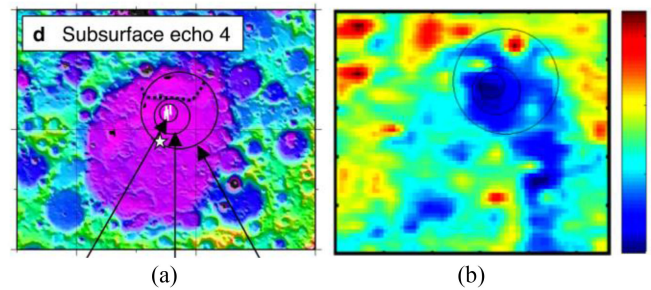


Fig. 10. (a) Spatial distribution of subsurface boundaries revealed by Ishiyama and Kumamoto [8]. The background image is lunar topography. The black circles (wide, intermediate, and narrow circles) show the areas of each subsurface boundary. (b) dTB map of mare Smythii at 37 GHz with the three subsurface boundaries vectorized and overlaid by black circles.

a strong correlation with the internal thermal activity of mare Smythii.

First, it is largely circular in shape, which is always related to the internal volcanic activity on Earth [29]. Additionally, Yingst and Head suggested that the northeast Em unit occurs in the region with the thinnest crust [1]. With a magma transport model, they suggested that plumes rising diapirically stall at a density boundary under the crust and propagate dikes to the surface through overpressurization in mare Smythii [1]. The area of the circular structure with abnormal substrate temperature is more than 90 km, which is likely related to the thinnest crust beneath the unit.

Moreover, with the SELENE LRS data, Ishiyama and Kumamoto identified four subsurface boundaries [8], three of which are displaced in Fig. 10(a). Also, the three subsurface boundaries are vectorized and then overlaid on the dTB map at 37 GHz. Fig. 10(b) shows that the narrow circle agrees well with the dTB anomaly with the lowest values, the intermediate circle largely agrees with the warm TB anomaly at night, and the wide circle agrees well with the west boundary of the regions with the relatively lower dTB.

The strong correlation between the LRS results and the CELMS findings indicates the similar important applications of the two datasets in exploring the basaltic volcanism of the Moon.

Second, the procurement of the LRO wide angle camera (WAC) image with high spatial resolution makes it possible to better understand the surface geological features of the mare basalts compared to the Clementine UV/VIS data used by Gillis and Spudis [3]. Based on the WAC image, we identified abundant wrinkle ridges occurred in the northeast Em unit [see Fig. 11(a)]. Clearly, these ridges are just located in the northeast boundary of the TB and dTB anomaly as shown in Fig. 11(b). The strong correlation between the TB and dTB anomaly and the LRS results and the wrinkle ridges brings about new clues to pursue the origin of the lava basalts in mare Smythii.

Further, the optical image presents 12 craters with floor fractures within mare Smythii, and this density is almost highest over the lunar surface [1], [3]. The extensive occurrences of the floor fractures imply the strong volcanic activity beneath Smythii basin. Combined with the special findings discussed above, the

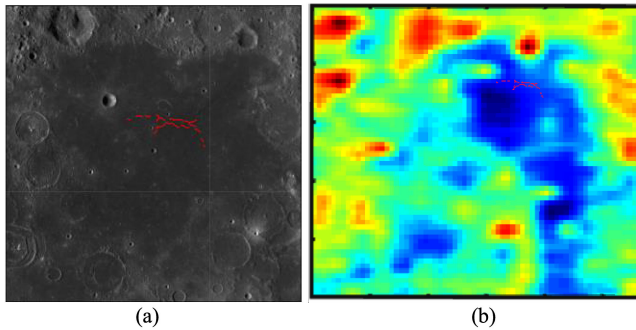


Fig. 11. Recognized wrinkle ridges based on (a) the WAC image indicated by red lines and (b) the ridges overlaid on the 37-GHz dTB map.

CE-2 CELMS data indicate a probable new method to explore the basaltic volcanism and thermal evolution of the Moon.

V. CONCLUSION

In this article, the CE-2 CELMS data were employed to assess the thermophysical characteristics of the floor materials in mare Smythii. Based on the theoretical simulation and the geological results by Gillis and Spudis [1], several special findings of the thermophysical features of the floor materials are proposed.

- 1) The TB at night in Em unit with the highest FTA is highest compared to the deposits with lower FTA, which was opposite to the theoretical simulation. Thus, we hypothesized and validated that the substrate temperature in Em unit of mare Smythii should be very high. Also, the substrate temperature in Smythii floor was abnormally high as a whole for the similar abnormal TB performances.
- 2) The four-channel TB and dTB maps indicate the apparent variation of the thermophysical parameters of volumetric regolith with depth in Em unit. Moreover, the comparatively lower daytime TB and dTB at 37 GHz hints that there is an unrevealed material in the upper layer of the regolith in Em unit, which has a strong thermal absorption ability. The dTB maps postulate that the region with the special material occurs in the eastern part of the basin floor, and it extends from the southeastern boundary of mare Smythii to the northern boundary.
- 3) The distribution of the TB and dTB anomaly shows a strong correlation with the subsurface boundaries identified by Ishiyama and Kumamoto (2019) with the LRS data. Moreover, there exist abundant wrinkle ridges in the northeast boundary of the TB anomaly. This means that the CELMS probably brings a potential new method to pursue the geological characteristics of the mare basalts.

However, the CELMS data do not have the ability to identify the special material existed in the upper layer of Em unit. More work deserved to be done to further explore the potentially geological applications of the microwave sounder data, though the CE-2 mission was ended in ten years ago.

ACKNOWLEDGMENT

The authors express their thanks to the people who help with this article. The UV/VIS data were downloaded from

http://webgis.wr.usgs.gov/pigwad/down/moon_dl.htm and the WAC data were downloaded from <http://wms.lroc.asu.edu/lroc/search>.

REFERENCES

- [1] R. A. Yingst and J. W. Head, III, "Characteristics of lunar mare deposits in Smythii and marginis basins: Implications for magma transport mechanisms," *J. Geophys. Res., Planets*, vol. 103, no. E5, pp. 11135–11158, 1998.
- [2] J. Conca and N. Hubbard, "Evidence for early volcanism in mare Smythii," in *Proc. Tenth Lunar Planet. Sci. Conf.*, 1979, pp. 1727–1737.
- [3] J. J. Gillis and P. D. Spudis, "Geology of the Smythii and marginis region of the moon: Using integrated remotely sensed data," *J. Geophys. Res., Planets*, vol. 105, no. E2, pp. 4217–4233, 2000.
- [4] P. D. Spudis and L. L. Hood, "Geological and geophysical field investigations from a lunar base at mare Smythii," in *Proc. NASA Conf. Publication*, 1992, pp. 163–163.
- [5] S. Nozette *et al.*, "The clementine mission to the moon: Scientific overview," *Science*, vol. 266, no. 5192, pp. 1835–1839, 1994.
- [6] P. D. Spudis and L. L. Hood, "Geological and geophysical investigations from a lunar base at mars Smythii," in *Proc. 2nd Conf. Lunar Bases Space Activities 21st Century*, 1988, pp. 163–174.
- [7] D. E. Wilhelms, F. John, and N. J. Trask, "The geologic history of the moon," 1987.
- [8] K. Ishiyama and A. Kumamoto, "Volcanic history in the Smythii basin based on SELENE radar observation," *Sci. Rep.*, vol. 9, no. 1, pp. 1–10, 2019.
- [9] B. A. Campbell *et al.*, "Volcanic and impact deposits of the moon's aristarchus plateau: A new view from earth-based radar images," *Geology*, vol. 36, no. 2, pp. 135–138, 2008.
- [10] Y. C. Zheng *et al.*, "Analysis of chang'e-2 brightness temperature data and production of high spatial resolution microwave maps of the moon," *Icarus*, vol. 319, pp. 627–644, 2019.
- [11] Z. G. Meng *et al.*, "Reevaluating mare moscoviense and its vicinity using chang'e-2 microwave sounder data," *Remote Sens.*, vol. 12, no. 3, 2020, Art. no. 535.
- [12] S. J. Keihm, "Effects of subsurface volume scattering on the lunar microwave brightness temperature spectrum," *Icarus*, vol. 52, no. 3, pp. 570–584, 1982.
- [13] T. Fang and W. Z. Fa, "High frequency thermal emission from the lunar surface and near surface temperature of the moon from chang'e-2 microwave radiometer," *Icarus*, vol. 232, pp. 34–53, 2014.
- [14] Y. C. Zheng *et al.*, "First microwave map of the moon with chang'e-1 data: The role of local time in global imaging," *Icarus*, vol. 219, no. 1, pp. 194–210, 2012.
- [15] Z. G. Meng *et al.*, "Thermophysical features of shallow lunar crust demonstrated by typical copernican craters using CE-2 CELMS data," *IEEE J. Sel. Topics Appl. Earth Observ. Remote Sens.*, vol. 12, no. 7, pp. 2565–2574, Jul. 2019.
- [16] Z. G. Meng *et al.*, "Internal structures of highlands in western lunar farside revealed by CE-2 CELMS data," *IEEE J. Sel. Topics Appl. Earth Observ. Remote Sens.*, vol. 13, no. 7, pp. 4859–4868, Aug. 2020.
- [17] G. P. Hu, K. L. Chan, Y. C. Zheng, and A. A. Xu, "A rock model for the cold and hot spots in the Chang'E microwave brightness temperature map," *IEEE Trans. Geosci. Remote*, vol. 56, no. 9, pp. 5471–5480, Sep. 2018.
- [18] K. L. Chan *et al.*, "Lunar regolith thermal behavior revealed by chang'e-1 microwave brightness temperature data," *Earth Planet. Sci. Lett.*, vol. 295, no. 1/2, pp. 287–291, 2010.
- [19] Z. G. Meng, S. Hu, T. Wang, C. Li, Z. Cai, and J. Ping, "Passive microwave probing mare basalts in mare imbrium using CE-2 CELMS data," *IEEE J. Sel. Topics Appl. Earth Observ. Remote Sens.*, vol. 11, no. 9, pp. 3097–3104, Sep. 2018.
- [20] Z. G. Meng *et al.*, "Influence of lunar topography on simulated surface temperature," *Adv. Space Res.*, vol. 54, no. 10, pp. 2131–2139, 2014.
- [21] Z. G. Meng, Q. Wang, H. Wang, T. Wang, and Z. Cai, "Potential geologic significances of hertzsprung basin revealed by CE-2 CELMS data," *IEEE J. Sel. Topics Appl. Earth Observ. Remote Sens.*, vol. 11, no. 10, pp. 3713–3720, Oct. 2018.
- [22] Z. C. Cai and T. Lan, "Lunar brightness temperature model based on the microwave radiometer data of chang'e-2," *IEEE Trans. Geosci. Remote Sens.*, vol. 55, no. 10, pp. 5944–5955, Oct. 2017.

- [23] Z. G. Meng *et al.*, “MTE features of apollo basin and its significance in understanding the SPA basin,” *IEEE J. Sel. Topics Appl. Earth Observ. Remote Sens.*, vol. 12, no. 7, pp. 2575–2583, Jul. 2019.
- [24] Z. G. Meng *et al.*, “Mare deposits identification and feature analysis in mare australe based on CE-2 CELMS data,” *J. Geophys. Res., Planets*, vol. 125, no. 7, 2020, Art. no. e2019JE006330.
- [25] P. G. Lucey, D. T. Blewett, and B. L. Jolliff, “Lunar iron and titanium abundance algorithms based on final processing of clementine ultraviolet/visible images,” *J. Geophys. Res., Planets*, vol. 105, no. E8, pp. 20297–20305, 2000.
- [26] Z. G. Meng *et al.*, “Complex mare deposits revealed by CE-2 CELMS data in mare nubium,” *IEEE J. Sel. Topics Appl. Earth Observ. Remote Sens.*, vol. 13, no. 1, pp. 2475–2484, May 2020.
- [27] Z. G. Meng, J. D. Zhang, Z. S. Tang, and Z. -S. Tang, “Microwave thermal emission features of mare orientale revealed by CELMS data,” *IEEE J. Sel. Topics Appl. Earth Observ. Remote Sens.*, vol. 10, no. 6, pp. 2991–2998, Jun. 2017.
- [28] Z. G. Meng *et al.*, “Influence of (FeO+TiO₂) abundance on the microwave thermal emissions of lunar regolith,” *Sci. China Earth Sci.*, vol. 59, no. 7, pp. 1498–1507, 2016.
- [29] Y. Y. Liu, *Remote Sensing Geology*, Beijing, China: Geolog. Publ. House, 2010.

Cai Liu received the Ph.D. degrees in geo-exploration and information technology from Jilin University, Changchun, China, in 1999.

From 1996 to 2000, he was an Associate Professor with Jilin University, where he became a Professor in 2000 and a Distinguished Professor of Jilin, China, in 2008. From 2004 to 2017, he was the Director of the College of Geo-Exploration Science and Technology, Jilin University. Since 2018, he has been with the 10 000 Talent Program. His research interest is the integrated research of geophysics and geology.

Liansheng Mei is currently working toward the master’s degree in solid geophysics with the College of Geoexploration Science and Technology, Jilin University, Changchun, China.

His research interests include application of microwave remote sensing technology in the planetary science and land surface parameters inversion using remote sensing technology and solid geophysics knowledge.

Zhiguo Meng (Member, IEEE) received the Ph.D. degree in solid geophysics from Jilin University, Changchun, China, in 2008.

He is currently a Professor with the College of Geoexploration Science and Technology, Jilin University. He has authored and coauthored more than 70 scientific papers. His research interests include the application and development of microwave remote sensing technology in the planetary science, primarily the microwave measurement of the lunar regolith.

Yongzhi Wang received the Ph.D. degree in geoexploration and information technology from Jilin University, Changchun, China, in 2008.

He is currently a Professor with the College of Geoexploration Science and Technology, Jilin University. From 2015 to 2016, he was a Visiting Scholar with York University, Toronto, ON, Canada. He has authored and coauthored more than 50 scientific papers. His research interests include remote sensing, geoscience big data, and artificial intelligence.

Dr. Wang is a Member of the International Association for Mathematical Geosciences.

Kai Zhu received the Ph.D. degree in structural geology from Jilin University, Changchun, China, in 2016.

He is currently a Research Associate with the Center for Lunar and Planetary Sciences, Institute of Geochemistry, Chinese Academy of Sciences. His research interests include lunar tectonics and structures.

Weiming Cheng received the Ph.D. degree in cartography and geographical information system from the State Key Laboratory of Resources and Environmental Information System, Institute of Geographic Sciences and Natural Resources Research, Chinese Academy of Science, Beijing, China, in 2003.

He is currently a Professor with the Institute of Geographic Sciences and Natural Resources Research, Chinese Academy of Sciences. His research interests include digital geomorphologic analysis, information extraction, digital geomorphologic mapping, and geomorphologic basic application research of ecoenvironmental change.

Zhanchuan Cai (Senior Member, IEEE) received the Ph.D. degree from Sun Yat-sen University, Guangzhou, China, in 2007.

From 2007 to 2008, he was a Visiting Scholar with the University of Nevada at Las Vegas, NV, USA. He is currently a Professor with the Faculty of Information Technology, Macau University of Science and Technology, Macau, China, where he is also with the State Key Laboratory of Lunar and Planetary Sciences, Macau University of Science and Technology, Macau. His research interests include remote sensing data processing and analysis, intelligent information processing, image processing and computer graphics, and multimedia information security.

Prof. Cai is also a Member of the Association for Computing Machinery, the Chang’e-3 Scientific Data Research and Application Core Team, and the Asia Graphics Association. He is also a Distinguished Member of the China Computer Federation. He was a recipient of the Third Prize of the Macau Science and Technology Award-Natural Science Award in 2012, the BOC Excellent Research Award from Macau University of Science and Technology in 2016, the Third Prize of the Macau Science and Technology Award-Technological Invention Award in 2018, and the Second Prize of the Teaching Achievement Award from Macau University of Science and Technology in 2020.

Jinsong Ping received the Ph.D. degree in astronomy from Shanghai Astronomical Observatories, Chinese Academy of Sciences, Shanghai, China, in 1996.

He is currently a Researcher in National Astronomical Observatories, Chinese Academy of Sciences, Beijing, China. His research interests include physics and dynamics for moons and planets, radio astrometry, and modeling the ionospheres for the earth and Mars with earth-based data.

Dr. Ping is a Member of Division A Fundamental Astronomy, Division B Facilities, Technologies and Data Science, Division E Sun and Heliosphere, Division F Planetary Systems and Bioastronomy, and Inter-Division A-F WG Cartographic Coordinates and Rotational Elements.

Alexander Gusev received the Ph.D. degree in physics from the Faculty of Physics, Moscow State University, Moscow, USSR, in 1981.

From 2004 to 2005, he was Invited Professor of NAOJ, Mizusawa VLBI observatory, Tokyo, Japan. From 2014 to 2015, he was Invited Professor of NAOC CAS, Beijing, China. He is currently a Senior Scientist and Associate Professor with the Department of Geophysics, Institute of Geology, Kazan Federal University, Kazan, Russia. He has authored and coauthored more than 180 scientific papers. His research interests include investigations of interior structure and dynamics for the Moon, pulsars, planetary data processing and analysis and ranging. Dr. Gusev is Academician, Full Member of the Russian Academy of Cosmonautics named Konstantin E. Tsiolkovsky, Russia, from 2019. He is a Member of Division A “Fundamental Astronomy” and a Member of Commission A2 “Rotation of the Earth” of IAU.